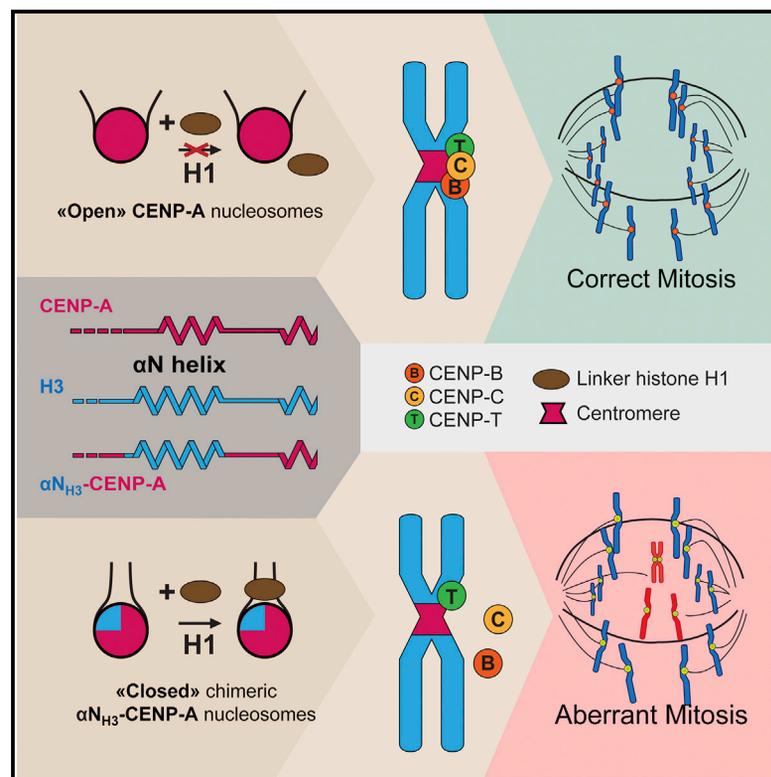# The Flexible Ends of CENP-A Nucleosome Are Required for Mitotic Fidelity

Graphical Abstract

Authors

Yohan Roulland, Khalid Ouararhni,
Mladen Naidenov, ..., Dimitar Angelov,
Ali Hamiche, Stefan Dimitrov

Correspondence

dimitar.anguelov@ens-lyon.fr (D.A.),
hamiche@igbmc.fr (A.H.),
stefan.dimitrov@univ-grenoble-alpes.fr
(S.D.)

In Brief

In this issue of *Molecular Cell*, Roulland
et al. describe the structural features of a
CENP-A nucleosome and identify the
mechanism by which its flexible DNA
arms interfere with linker histone H1
recruitment, assist active kinetochore
assembly, and ensure mitotic fidelity.

Highlights

- CENP-A nucleosomal ends are highly flexible in solution

- Dynamic CENP-A nucleosomal ends prevent H1 recruitment

- Flexibility of DNA ends allows active kinetochore complex assembly

- Open CENP-A nucleosomal structure is essential for its mitotic function

CrossMark

CellPress

The Flexible Ends of CENP-A Nucleosome Are Required for Mitotic Fidelity

Yohan Roulland,[1] Khalid Ouararhni,[2] Mladen Naidenov,[3,9] Lorrie Ramos,[1] Muhammad Shuaib,[2] Sajad Hussain Syed,[1,3,10] Imtiaz Nizar Lone,[1,3] Ramachandran Boopathi,[1,3] Emeline Fontaine,[1] Gabor Papai,[4] Hiroaki Tachiwana,[5] Thierry Gautier,[1] Dimitrios Skoufias,[6] Kiran Padmanabhan,[7] Jan Bednar,[1] Hitoshi Kurumizaka,[5] Patrick Schultz,[4] Dimitar Angelov,[3,*] Ali Hamiche,[2,8,*] and Stefan Dimitrov[1,*]

[1]Université de Grenoble Alpes/INSERM U1209/CNRS UMR 5309, 38042 Grenoble Cedex 9, France
[2]Department of Functional Genomics and Cancer, Institut de Génétique et Biologie Moléculaire et Cellulaire (IGBMC), Equipe Labellisée Ligue Contre le Cancer/Université de Strasbourg/CNRS/INSERM, 67404 Illkirch Cedex, France
[3]Laboratoire de Biologie Moléculaire de la Cellule (LBMC) CNRS/ENSL/UCBL UMR 5239 and Institut NeuroMyoGène – INMG CNRS/UCBL UMR 5310, Université de Lyon, Ecole Normale Supérieure de Lyon, 69007 Lyon, France
[4]Department of Integrated Structural Biology, Institut de Génétique et Biologie Moléculaire et Cellulaire (IGBMC)/Université de Strasbourg/CNRS/INSERM, 67404 Illkirch Cedex, France
[5]Laboratory of Structural Biology, Graduate School of Advanced Science and Engineering, Waseda University, Shinjuku, Tokyo 162-8480, Japan
[6]Institut de Biologie Structurale, Université de Grenoble Alpes, 38044 Grenoble, France
[7]Institut de Génomique Fonctionnelle de Lyon, Ecole Normale Supérieure de Lyon, Centre National de la Recherche Scientifique, UMR 5242, 46 Allée d'Italie, 69364 Lyon Cedex 07, France
[8]Qatar Biomedical Research Institute, Hamad Bin Khalifa University, P.O. Box 5825, Qatar Foundation, Doha, Qatar
[9]Present address: Department of Plant Physiology and Molecular Biology, University of Plovdiv, Faculty of Biology, Plovdiv 4000, Bulgaria
[10]Present address: Division of Cancer Pharmacology, Indian Institute of Integrative Medicine (CSIR), Jammu 180001 and Kashmir, India
*Correspondence: dimitar.anguelov@ens-lyon.fr (D.A.), hamiche@igbmc.fr (A.H.), stefan.dimitrov@univ-grenoble-alpes.fr (S.D.)
http://dx.doi.org/10.1016/j.molcel.2016.06.023

SUMMARY

CENP-A is a histone variant, which replaces histone H3 at centromeres and confers unique properties to centromeric chromatin. The crystal structure of CENP-A nucleosome suggests flexible nucleosomal DNA ends, but their dynamics in solution remains elusive and their implication in centromere function is unknown. Using electron cryo-microscopy, we determined the dynamic solution properties of the CENP-A nucleosome. Our biochemical, proteomic, and genetic data reveal that higher flexibility of DNA ends impairs histone H1 binding to the CENP-A nucleosome. Substituting the 2-turn αN-helix of CENP-A with the 3-turn αN-helix of H3 results in compact particles with rigidified DNA ends, able to bind histone H1. In vivo replacement of CENP-A with H3-CENP-A hybrid nucleosomes leads to H1 recruitment, delocalization of kinetochore proteins, and significant mitotic and cytokinesis defects. Our data reveal that the evolutionarily conserved flexible ends of the CENP-A nucleosomes are essential to ensure the fidelity of the mitotic pathway.

INTRODUCTION

Chromatin is composed of repetitive structures of the basic unit, a nucleosome, which consists of histone octamer composed of core histones (two of each H2A, H2B, H3, and H4) around which 167 base pairs (bp) of DNA are wrapped to form two superhelices (Luger et al., 1997; Van Holde et al., 1980). Individual nucleosomes interspersed with linker DNA form the 10 nm chromatin filament (Thoma et al., 1979; Van Holde et al., 1980). A fifth histone, termed "linker histone", interacts with this linker DNA and assists in the assembly, condensation, and stability of the 30 nm chromatin fiber (Makarov et al., 1983; Thoma et al., 1979).

In addition to the conventional core histones, each cell expresses histone variants. Histone variants are non-allelic isoforms of conventional histones and all histones, except H4, have variants (Van Holde et al., 1980). Incorporation of these variants confers novel structural and functional properties to chromatin (reviewed in Boulard et al., 2007).

The histone CENP-A is a textbook example of a histone variant that upon incorporation changes the properties of a nucleosome (Goutte-Gattat et al., 2013; Kingston et al., 2011; Mizuguchi et al., 2007; Tachiwana et al., 2011). CENP-A belongs to the H3 family of histones (Earnshaw and Migeon, 1985; Palmer et al., 1987) and is exclusively localized to centromeres and defines the specific centromere structure and function (Buscaino et al., 2010).

CENP-A epigenetically marks the centromeres, where it is required for the assembly of active kinetochores. The constitutive centromere associated network (CCAN), a complex consisting of 16 proteins (termed generally as CENPs), recognizes and directly interacts with centromeric chromatin (Perpelescu and Fukagawa, 2011). Importantly, two of the CCAN members, CENP-C and CENP-T, assemble a platform to direct kinetochore formation (Perpelescu and Fukagawa, 2011).
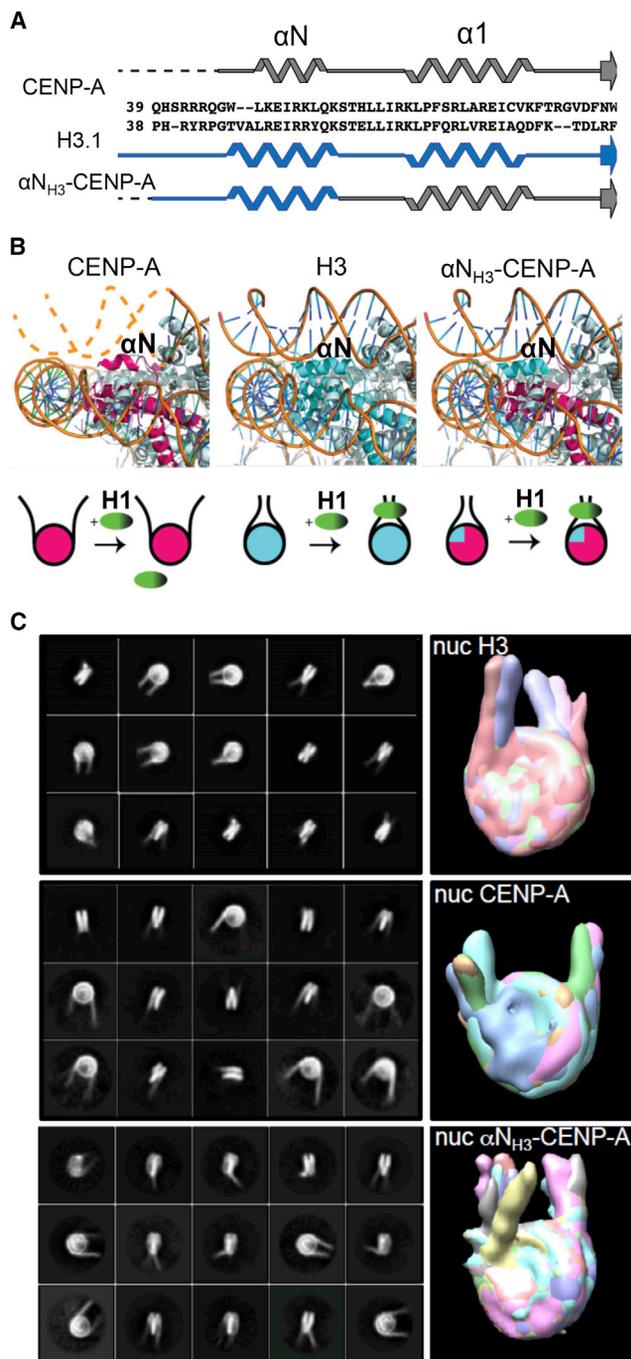
CrossMark

A

B

C

CENP-A depletion results in numerous mitotic and cytokinetic defects and subsequent aneuploidy (Goutte-Gattat et al., 2013; Régnier et al., 2005). CENP-A loss leads to altered composition and organization of the kinetochore, including the delocalization of the inner kinetochore proteins CENP-C, CENP-I, and CENP-H as well as the outer kinetochore components HEC1, Mad2, and CENP-E (Goutte-Gattat et al., 2013; Régnier et al., 2005).

The crystal structure of the CENP-A nucleosome particle was recently solved (Tachiwana et al., 2011). In contrast to the conventional nucleosome structure, only 121 bp of DNA are resolved in the crystal structure of the CENP-A nucleosome, suggesting that 13 bp of DNA at each nucleosomal end display marked flexibility. In agreement with this suggestion, CENP-A nucleosomal ends exhibited higher accessibility to nucleases (Kingston et al., 2011). Experiments in solution point to some crystal packing artifacts, which might affect the central part of the CENP-A nucleosomes, but not the dynamics of their ends (Falk et al., 2015). However, whether the CENP-A driven nucleosomal end DNA flexibility has any physiological consequences is totally unknown.

To determine the dynamics of nucleosomal DNA ends in solution, both conventional and CENP-A nucleosomes were analyzed by using electron cryomicroscopy (ECM) combined with 3D reconstruction. ECM data clearly show that the CENP-A nucleosomal ends, as suggested by the crystal structure, exhibit a high degree of flexibility. The αN helix of H3 and the preceding loop, which is in contact with DNA, plays a role in stabilizing the conventional nucleosomal DNA ends. This specific rigid orientation of the exit and entry angle of the nucleosomal DNA ends, in addition to the linker histone H1 binding modes and condensation of nucleosomal arrays, is regulating the interaction of H1 with conventional nucleosomes (Song et al., 2014; Syed et al., 2010; Zhou et al., 2013; Zhou et al., 2015). Thus, highly dynamic CENP-A nucleosomal ends would likely preclude the binding of H1, which might in turn be important for centromere function and kinetochore assembly (Figures 1A and 1B). Since the fixed entry/exit angle and rigidity of DNA ends of conventional nucleosome are governed by the interaction of the αN helix of H3, we created a hybrid CENP-A nucleosome, wherein the αN helix of CENP-A was replaced with that of H3, which is one helical turn longer. ECM analysis reveals that this hybrid H3-CENP-A particle, in contrast to the wild-type (WT) CENP-A nucleosome, exhibits a compact structure very similar to that of the conventional nucleosome. We then studied the properties of these hybrid nucleosomes in vitro and in vivo and compared them with those of the WT CENP-A nucleosomes. Our biochemical and cell biological data demonstrate that the flexible DNA ends of CENP-A nucleosome are essential for the structural integrity of the centromere, which is required for the fidelity of the mitotic process.

Figure 1. The Hybrid αN$_{H3}$-CENP-A Nucleosome, in Contrast to the WT CENP-A Nucleosome, Exhibits a Compact Structure Very Similar to that of the Conventional Nucleosome

(A) Schematics of the secondary structure of the N-terminal regions of CENP-A, H3, and αN$_{H3}$-CENP-A in the nucleosome. The sequences of human CENP-A, H3, and αN$_{H3}$-CENP-A are aligned with the secondary structural elements.

(B) Close up views of the αN helices and the DNA edge regions of CENP-A (left) and H3 (middle) nucleosomes; right, predicted organization of the αN helices and the DNA edge regions of αN$_{H3}$-CENP-A nucleosome; bottom, schematics of the expected interaction of H1 with the respective nucleosomes, depicted in the upper images.

(C) ECM and image analysis of conventional, CENP-A, and mutant αN$_{H3}$-CENP-A nucleosomes reconstituted on 601 DNA; gallery of class averages after image alignment and clustering for conventional (upper), CENP-A (middle), and αN$_{H3}$-CENP-A (lower) nucleosomes without H1; right, surface representation of the main distinct conformations of conventional (upper), CENP-A (middle), and αN$_{H3}$-CENP-A (lower) nucleosomes.

RESULTS

CENP-A Nucleosomes Exhibit Highly Dynamical DNA Ends in Solution, Determined by the "Defective" αN Helix of CENP-A

We used ECM to analyze the dynamics of CENP-A nucleosome in solution. We purified recombinant human core histone octamers containing conventional H3 or CENP-A (Figure S1) and reconstituted centrally positioned nucleosomes on 197 bp 601 DNA in order to have 25 bp free DNA ends. The reconstituted particles were studied in frozen hydrated conditions (Figure S2). Frames showing well-separated nucleosomes were selected and 29,711 and 24,286 molecular images were extracted for conventional and CENP-A nucleosomes, respectively. These images were used for building ab initio a 3D model of the particles (Figure 1C). The final ECM map is in full agreement with the crystal structure of the nucleosome core particle (NCP) (Luger et al., 1997). To analyze the conformational variability of the particle population, a 3D classification scheme based on maximum likelihood optimization was used to separate different structural variants (Scheres, 2012; Table S1). While the nucleosome core showed little variation, we observed distinct configurations of the DNA ends for both conventional and CENP-A particles (Figure 1C). For each 3D class, the angles between each linker arm and the dyad axis were determined in the front and the site view of the nucleosome (Figure S3). The analyses indicated that, in particular, the CENP-A particles have open conformations with much higher entry/exit angles (higher DNA end orientation fluctuations) compared to the conventional ones. We conclude that in solution, the CENP-A nucleosomal ends exhibited, as suggested by the X-ray diffraction studies, a very high degree of flexibility. The αN helix of CENP-A is one helical turn shorter than that of conventional H3 nucleosome and the preceding region, in contrast to that of H3, is completely disordered (Tachiwana et al., 2011; see also Figure 1B). However, both the αN helix length and the loop segment preceding the αN helix (which directly interacts with the DNA ends in H3 nucleosome; Luger et al., 1997) are required for maintaining the DNA orientation at the entrance and exit of H3 nucleosomes. Thus, the specific organization of these regions in CENP-A might be responsible for the inherent flexibility of the DNA ends of the CENP-A nucleosome (Tachiwana et al., 2011; Figure 1B). Therefore, we hypothesized that swapping the CENP-A αN helix and the segment preceding it with those of conventional H3 would rigidify the ends of nucleosomal CENP-A DNA. To test this, we generated a hybrid H3-CENP-A mutant (αNH3-CENP-A) containing the αN helix and the preceding loop region of H3. Next, we expressed this construct in bacteria and, after purification, we used it for reconstitution of αNH3-CENP-A nucleosomes on 197 bp 601 DNA (Figure S1). The structure and dynamics of the mutant αNH3-CENP-A nucleosomes were studied by ECM as described above for both conventional and CENP-A nucleosome. There were 155,000 molecular images that were extracted and used for building ab initio a 3D model of the hybrid particles (Figures 1C, bottom, S2 and S3). As seen, the mutant αNH3-CENP-A particle exhibits a structure very similar to those of conventional H3 nucleosome conformations, with smaller entry/exit angles of the DNA ends. Therefore, the defective αN helix

of CENP-A is the main determinant for the highly flexible CENP-A nucleosomal ends.

CENP-A Nucleosome Is Refractive to Histone H1 Binding

The binding of histone H1 to the nucleosome is regulated by the entry/exit angle of the nucleosomal DNA ends and is favored by rigid DNA (Bednar et al., 1998; Syed et al., 2010). The flexibility of the ends within the CENP-A nucleosome might therefore interfere with the binding of histone H1. To analyze the ability of histone H1 to interact in vitro with the CENP-A nucleosome, we have used a combination of two techniques, namely electro-mobility shift assay (EMSA) and hydroxyl radical (·OH) footprinting. EMSA allows the visualization of H1 binding to the nucleosome, but does not differentiate between specific and non-specific association, while ·OH footprinting detects the specific H1 binding at 1 bp resolution (Menoni et al., 2012; Syed et al., 2010).

A physiologically relevant linker histone chaperone (NAP-1) was used to deposit histone H1 on centrally positioned conventional or CENP-A nucleosomes (Syed et al., 2010). The particle solutions were incubated with increasing amounts of NAP-1/H1 complex and run on native PAGE (Figure 2A). As seen, at the NAP-1/H1 concentration, when a complete shift for the H3-nucleosome was found, only a very weak shifted band reflecting the H1-CENP-A-nucleosomal complex was detected. These data showed that the presence of CENP-A interferes with the binding of histone H1 to the nucleosome.

The ·OH footprinting patterns of conventional and CENP-A di-nucleosome were very similar; i.e., no enhanced cleavage at the DNA ends of the CENP-A nucleosome was observed (Figure 2B). This reflects the lack of sensitivity of the method to detect the dynamics and the transient dissociation of the ends from the core histone octamer. Some perturbations (increase of the ·OH cleavage "noise") in the ·OH cleavage pattern can be observed only when the DNA nucleosomal ends are permanently and completely dissociated from the histone octamer as in the case of the histone variant H2A.Bbd and the chimeric H2A.ddBbd nucleosomes (see Figures 4 and S1; Shukla et al., 2011).

In agreement with our earlier data (Syed et al., 2010), the binding of histone H1 to conventional H3 di-nucleosomes results in: (1) clear protection of the nucleosomal dyad due to the strong interaction of the globular domain of H1 with the dyad, and (2) generation of 10 bp repeat of the linker DNA (Figure 2B, footprinting gel and the scans), which reflects the H1-induced formation of the stem structure (H1 interacts with both linkers and brings them in close vicinity and, thus, induces the assembly of the stem (Hamiche et al., 1996; Menoni et al., 2012; Syed et al., 2010). However, only very faint protection and 10 bp repeats were observed in CENP-A-di-nucleosomes incubated with the NAP1/H1 complex (Figure 2B, footprinting gel and the scans). These data revealed weak interaction of histone H1 with the CENP-A particles. Taken together, our in vitro experiments demonstrate that the CENP-A nucleosomal templates are poor substrates for H1 binding.

"Rigidifying" the DNA Ends of the CENP-A Nucleosome Allows Efficient Binding of Histone H1 In Vitro

A low degree of flexibility of the nucleosomal DNA ends is required for the efficient and specific binding of histone H1.
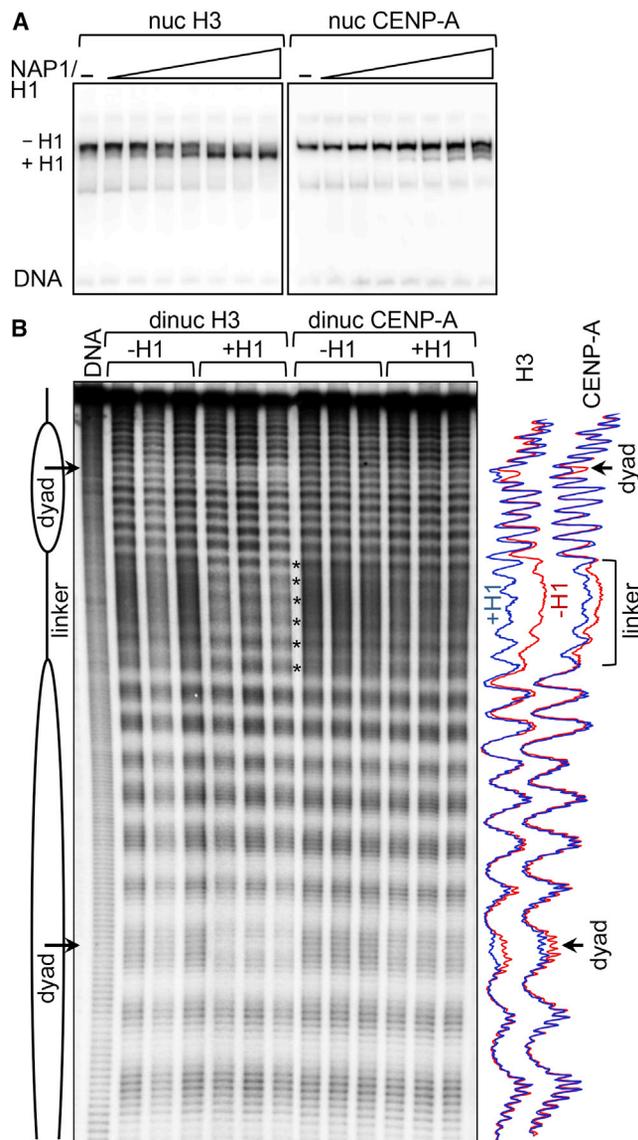
Figure 2. The Presence of CENP-A Interferes with Histone H1 Binding to the Nucleosome

(A) EMSA of binding of histone H1 to conventional H3 (nucH3, left) and to CENP-A (nuc CENP-A, right) mononucleosomes. The particles were incubated with increasing amounts of NAP-1-histone H1 complex.

(B) •OH footprinting of conventional H3 and CENP-A di-nucleosomes. The di-nucleosomes were assembled with H1 and H1 binding was analyzed by •OH footprinting. On the left are schematics of the di-nucleosome, the nucleosome dyad is indicated with an arrow, and on the right are scans of the •OH digestion pattern of H3 and CENP-A di-nucleosomes, assembled (+H1, blue) or not (−H1, red) with H1.

The swapped αN$_{H3}$-CENP-A mutant particle has rigid DNA ends (Figure 1C) as conventional H3 nucleosomes, and thus, would allow H1 binding (see schematics, Figures 1A and 1B). To test this, we analyzed the interaction of H1 with αN$_{H3}$-CENP-A nucleosomes with both EMSA and •OH footprinting as described for WT CENP-A (Figure 2). H1.5 subtype was used in these experiments. Of note, H1.5 exhibits very similar to H1.2 binding effi-

ciency to the nucleosome (Figure S4). The deposition of H1 was performed by using the NAP-1/H1 complex, as detailed in Figure 2. The EMSA experiment clearly shows that histone H1 binds to both H3 and αN$_{H3}$-CENP-A particles with the same efficiency (Figure 3A, compare upper and lower). •OH footprinting revealed identical localization of histone H1 on both control H3 and αN$_{H3}$-CENP-A nucleosomes as evidenced by a clear protection at the nucleosomal dyad and the generation of the typical •OH cleavage 10 bp-repeat of the linker DNA (Figure 3B). Therefore, the hybrid αN$_{H3}$-CENP-A nucleosomes, in contrast to WT CENP-A nucleosomes, are able, as predicted, to bind H1 with higher specificity and affinity.

H1 Is Not Associated with CENP-A Chromatin In Vivo

To determine whether H1 binding to CENP-A nucleosomes was also negatively affected in vivo as our in vitro experiments demonstrated, we used a proteomic approach coupled to mass spectrometry using cell culture models. We generated stable HeLa cell lines expressing double HA and FLAG tagged CENP-A (e-CENP-A) (Goutte-Gattat et al., 2013; Shuaib et al., 2010). Stable HeLa cell lines expressing double-tagged conventional histone H3.1 (e-H3.1) or the histone variant H3.3 (e-H3.3) were used as positive controls. We isolated the nucleosomal e-CENP-A as well as both e-H3.1 and e-H3.3 nucleosomal complexes by double immunoaffinity purification (Goutte-Gattat et al., 2013). The composition of the complexes was analyzed by mass spectrometry, SDS PAGE, and western blotting (Figure 4). The e-CENP-A complex, in agreement with the available data (Foltz et al., 2006; Goutte-Gattat et al., 2013), contained several proteins from the CCAN as well as other proteins (Figure 4; Table S2). Importantly, no histone H1 was found associated within the complex as shown by electrophoretic analysis, western blotting, and mass spectrometry (Figures 4B–4D), although e-H3.1 and e-H3.3 nucleosomal complexes contained both isoforms H1.1 and H1.2 of histone H1 (Figure 4A). Therefore, histone H1 does not associate in vivo with CENP-A chromatin. These in vivo data fully agree with the poor non-specific in vitro binding of H1 to reconstituted CENP-A nucleosomes (Figure 1).

In Vivo Binding of H1 to the αN$_{H3}$-CENP-A Nucleosome

Does artificially rigidifying CENP-A nucleosomal ends allow H1 binding in vivo? To analyze this, we generated stable HeLa cell lines expressing double HA and FLAG epitope tagged αN$_{H3}$-CENP-A. The αN$_{H3}$-CENP-A nucleosomal complex was purified as above and compared to the WT CENP-A nucleosomal complex. Its members were characterized by SDS PAGE, western blot, and mass spectrometry (Figures 4B–4D). Unlike the CENP-A nucleosomal complex, all methods identified histone H1 present in the αN$_{H3}$-CENP-A nucleosomal complex. The characteristic histone H1 doublet was present in the electrophoretic pattern of the αN$_{H3}$-CENP-A complex, but not in that of WT CENP-A one (Figure 4B). The anti-H1 antibody revealed a clear doublet corresponding to H1 (Figure 4C) and 15 H1 peptides (in total) were found by mass spectrometry in the αN$_{H3}$-CENP-A nucleosomal complex (Figure 4D). Taken as a whole, our data reveal that the swapping the αN helix, and the preceding region of CENP-A with those of H3, primarily drives the generation of a
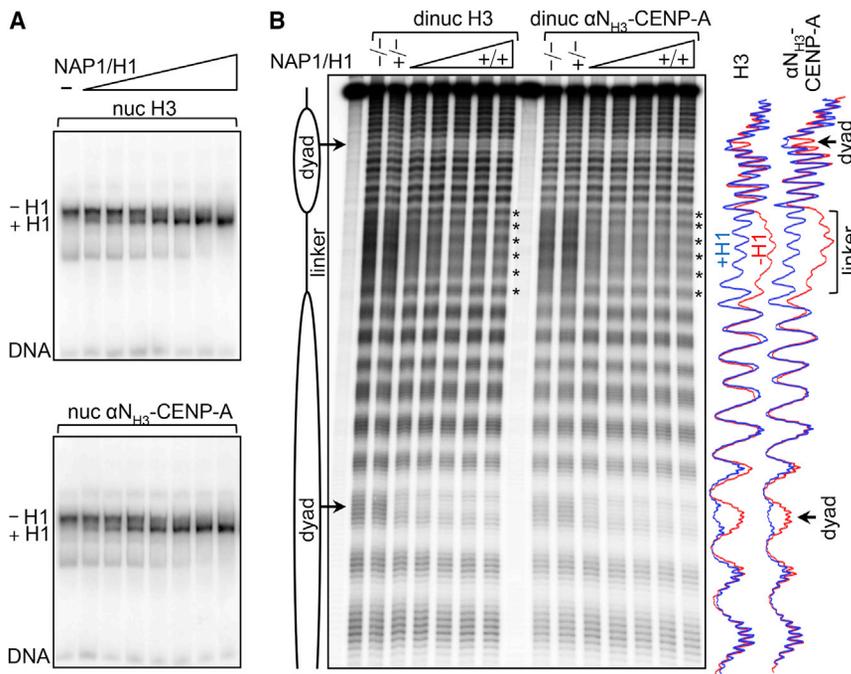
Figure 3. Efficient In Vitro Binding of Histone H1 Swapped αNH3 Helix Mutant CENP-A, αN$_{H3}$-CENP-A, Nucleosome

(A) EMSA of histone H1 binding to H3 and αN$_{H3}$-CENP-A nucleosomes. Conventional H3 (upper) or swapped αN$_{H3}$-CENP-A nucleosomes (lower) were incubated with increasing amounts of NAP-1-histone H1 complex and were analyzed by PAGE. The positions of the non-bound and H1-bound nucleosomes are indicated.

(B) ·OH footprinting of H3 and αN-H3-CENP-A di-nucleosomes. The di-nucleosomes were assembled with increasing amounts of NAP-1-histone H1 complex and H1 binding was analyzed by ·OH footprinting. On the left are schematics of the di-nucleosome, the nucleosome dyad is indicated with an arrow, and on the right are scans of the ·OH digestion pattern of H3 and CENP-A di-nucleosomes, assembled (+H1, blue) or not (−H1, red) with H1.

particle with rigid orientation of the entry/exit DNA ends, which then allows efficient and specific association with histone H1 both in vitro and in vivo.

The In Vivo Replacement of CENP-A with the αN$_{H3}$-CENP-A Swap Mutant Leads to Strong Mitotic and Cytokinetic Defects

A hybrid αN$_{H3}$-CENP-A with H1 bound to it would in turn lead to the formation of condensed chromatin fibers similar to those established with canonical H3. Could this compact structure of the αN$_{H3}$-CENP-A chromatin then affect the function of centromeres? To test this hypothesis, endogenous CENP-A was knocked down by using specific small interfering (si)RNAs in HeLa cell lines, and we analyzed the effect of expressing a siRNA resistant GFP-αN$_{H3}$-CENP-A hybrid transcript as compared to a siRNA resistant GFP-CENP-A transcript (see schematics in Figure 5A). This was followed by quantitative analysis of mitotic progression in all cell lines.

Treatment with siRNA results in very strong ablation of endogenous CENP-A: more than 85%–90% of endogenous CENP-A was depleted in each of the cell lines used and, as expected, the expression of the siRNA-resistant GFP-fusions was not affected (Figure 5B). Both GFP-fusions were found localized to the centromeres (Figure 5C). In agreement with the reported data (Goutte-Gattat et al., 2013; Régnier et al., 2005), the absence of CENP-A in naive HeLa cells has deleterious effects on both mitosis and cytokinesis (Figure 5C). CENP-A depleted cells exhibited numerous mitotic and cytokinetic defects including chromosome misalignment, lagging chromosomes, chromosome bridges, and multiple nuclei in interphase (Figures 5C–5E). The presence of stably expressed GFP-CENP-A completely rescued the mitotic and cytokinetic defects in HeLa cells lines treated with siRNA (Figures 5C–5E). No rescue

was, however, observed in CENP-A depleted HeLa cell lines stably expressing the GFP-αN$_{H3}$-CENP-A fusion (Figures 5C–5E).

HeLa cells are polyploid and exhibit some mitotic defects even under normal growth conditions and while our data clearly illustrate that cells harboring hybrid CENP-A nucleosomes are in a poor condition, we cannot rule out some off-target effects. To conclusively eliminate any possible undesirable effects, we established conditional homozygous knockout/knockin (cKO/KI) mouse lines, where the endogenous CENP-A was replaced with a HA-FLAG-tagged CENP-A version (Figure 6A). These mice did not show any visible phenotype and were fertile. We derived mouse embryonic fibroblasts (MEF) from 14.5 days post coitum embryos and immortalized them. The immortalized MEFs were transfected with constructs expressing a tamoxifen inducible Cre-ERT2 recombinase along with either GFP-CENP-A or GFP-αN$_{H3}$-CENP-A mutants and stable lines were established. Quantification of centromeres in over 100 cells indicated that the amount of both GFP-fusions incorporated at the centromeres of the respective MEFs were identical (Figure S5).

Tamoxifen induced Cre-ERT2 expression led to excision of both CENP-A alleles and subsequent depletion of CENP-A protein. Western blot analysis showed that 8 days after tamoxifen treatment, the endogenous protein was completely depleted (Figures 6B–6D) and a strong increase of both mitotic and cytokinesis defects were observed in the control CENP-A depleted MEFs (Figures 6E–6G). The expression of GFP-CENP-A was sufficient to completely rescue the phenotype (Figures 6E–6G). The expression of GFP-αN$_{H3}$-CENP-A, however, was unable to rescue both the mitotic and cytokinesis defects (Figures 6E–6G). In the absence of endogenous CENP-A, the stable MEFs expressing GFP-αN$_{H3}$-CENP-A exhibited close to 2-fold more mitotic defects compared to those expressing GFP-CENP-A (Figure 6F). Of note, GFP-αN$_{H3}$-CENP-A is likely to act as a dominant negative since its stable expression (in the presence of endogenous CENP-A) is associated with ~2-fold increase of
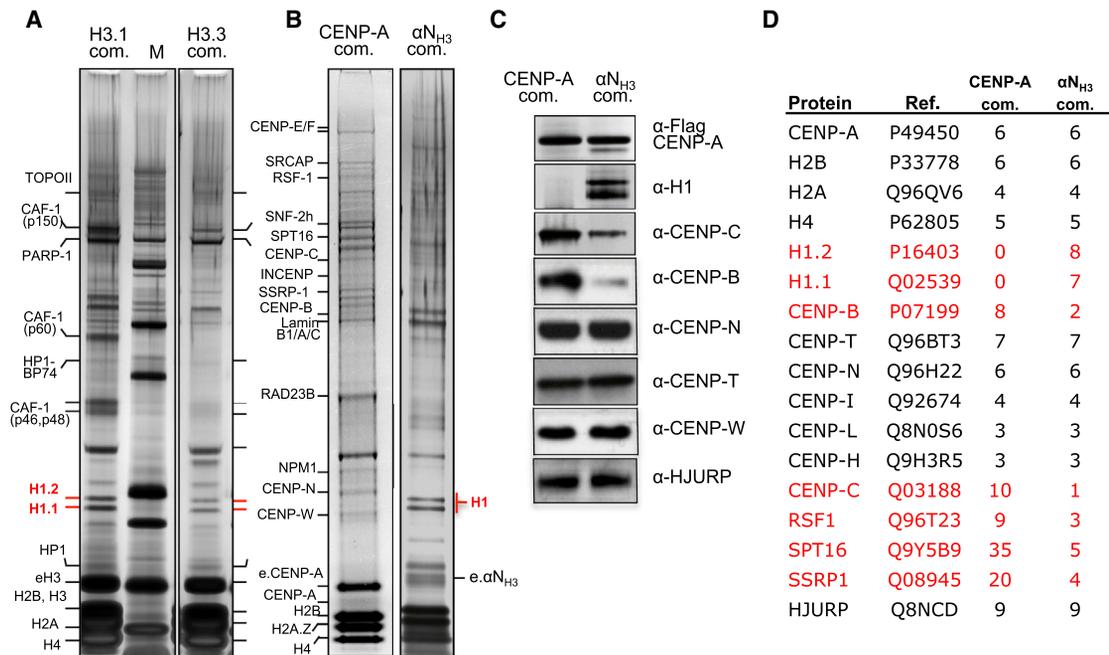
Figure 4. Histone H1 Binds In Vivo to the αN_H3-CENP-A Swapped Nucleosomes, but Not to WT CENP-A Particles

(A) Silver staining of proteins associated with either e-H3.1 or e-H3.3 nucleosomes. The nucleosomal e-H3.1 and e-H3.3 complexes were purified by tandem immunoaffinity from stable HeLa cells expressing either e-H3.1 or e-H3.3 and the associated polypeptides were identified by mass spectrometry. Lane M corresponds to a protein molecular mass marker. The H1 histones (both H1.1 and H1.2 isoforms) are indicated in red.

(B) Silver staining of proteins associated with either the e-CENP-A (left) or the e-αN_H3-CENP-A (right) nucleosomal complexes isolated from stable HeLa expressing either e-CENP-A or e-αN_H3-CENP-A, respectively. Note that the e-CENP-A complex, in contrast to e-αN-H3-CENP-A and both e-H3.1 and e-H3.3 complexes, is not associated with histone H1.

(C) Western blot detection of the indicated proteins associated with either the WT e-CENP-A or e-αN_H3-CENP-A mutant nucleosomes.

(D) Mass spectrometry analysis of selected proteins associated with either the WT e-CENP-A or e-αN_H3-CENP-A mutant nucleosomes. The proteins together with the number of identified peptides are shown. The proteins with distinct number of identified peptides in both complexes are indicated in red.

Protein	Ref.	CENP-A com.	αN_H3 com.
CENP-A	P49450	6	6
H2B	P33778	6	6
H2A	Q96QV6	4	4
H4	P62805	5	5
H1.2	P16403	0	8
H1.1	Q02539	0	7
CENP-B	P07199	8	2
CENP-T	Q96BT3	7	7
CENP-N	Q96H22	6	6
CENP-I	Q92674	4	4
CENP-L	Q8N0S6	3	3
CENP-H	Q9H3R5	3	3
CENP-C	Q03188	10	1
RSF1	Q96T23	9	3
SPT16	Q9Y5B9	35	5
SSRP1	Q08945	20	4
HJURP	Q8NCD	9	9

mitotic defects compared to these of control MEFs (Figure 6F). Taken as a whole, the data in both HeLa cells and in MEFs reveal that the replacement of CENP-A with αN_H3-CENP-A nucleosomes at the centromeres impairs both mitosis and cytokinesis in these cells.

Replacement of CENP-A with the Swapped αN_H3-CENP-A Mutant at the Centromeres Leads to Aberrant Localization of CENP-C

The deleterious effect of αN_H3-CENP-A hybrid nucleosomes on centromere function might reflect reduced amount or absence of some proteins from the CCAN complex, crucial for the assembly of active kinetochores. Comparative mass spectrometry analysis on the composition of αN_H3-CENP-A and the WT CENP-A nucleosomal complexes reveals that this is the case (Figure 4; Table S2). In agreement with earlier observations (Goutte-Gattat et al., 2013), the WT CENP-A nucleosomal complex comprised a large number of CCAN proteins (CENP-B, CENP-T, CENP-N, CENP-I, CENP-L, CENP-C, and CENP-H, etc.), the CENP-A chaperone HJURP, the chromatin remodeler RSF-1, as well as many other proteins (Figure 4; Table S2). These proteins are also members of the αN_H3-CENP-A nucleosomal complex (Figures 4C and 4D; Table S2). However, the number of identified peptides originating from several of the identified

proteins and in particular for both CENP-C and CENP-B, RSF-1, and the two subunits (SPT16 and SSRP1) of FACT dramatically decreased in the αN_H3-CENP-A nucleosomal complex compared to the WT CENP-A complex (Figure 4D; Table S2), suggesting a strong loss of these proteins in the αN_H3-CENP-A nucleosomal complex. Western blot analysis further confirmed that the amount of both CENP-C and CENP-B is much lower in the αN_H3-CENP-A nucleosomal complex (Figure 4C). In contrast, the levels of several CCAN proteins, including CENP-T, CENP-N, and CENP-W are not affected in both types of nucleosomes, as shown by western blot and mass spectrometry (Figures 4C and 4D). In addition, no changes in the HJURP associated with both the nucleosomal and the nuclear soluble GFP-CENP-A and GFP-αN_H3-CENP-A were observed (Figures 4C and S7B).

Indeed, immunofluorescence analysis of the localization of CENP-C in stable HeLa cells expressing αN_H3-CENP-A and depleted of endogenous CENP-A support our biochemical data (Figure 7). Depletion of CENP-A in naive HeLa cells results in dramatic delocalization of CENP-C, but not of CENP-T from the centromeres (Figures 7A, 7B, and S6). In the siRNA treated stable HeLa cells expressing GFP-CENP-A, this phenotype was completely rescued; i.e., a CENP-C centromere specific localization was indistinguishable from that observed in naive
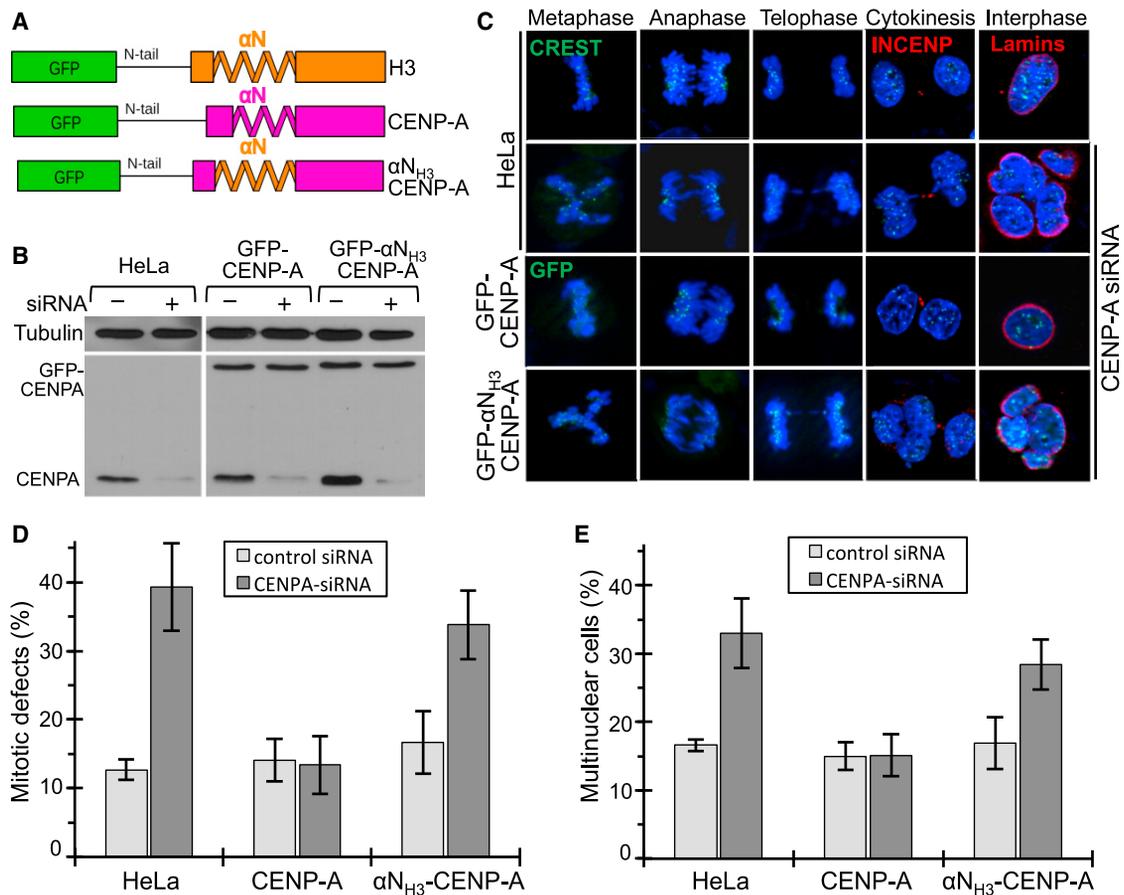
Molecular Cell 63, 674–685, August 18, 2016   679

Figure 5. The Replacement in HeLa Cells of WT CENP-A with the Swapped αN_{H3}-CENP-A Mutant at the Centromere Results in Strong Mitotic and Cytokinetic Defects

(A) Schematics for the silencing resistant GFP-fusions used for the in vivo replacement of WT CENP-A with the swapped αN_{H3}- CENP-A mutant.

(B) Western blot detection of the GFP-CENP-A fusions and endogenous CENP-A using anti-CENP-A antibody in cells treated with control siRNA (−) or CENP-A siRNA (+). The nuclear proteins were extracted 72 hr post-transfection. The cell lines as well as the positions of the GFP-CENP-A fusions and endogenous CENP-A are indicated.

(C) Cell-cycle visualization, after endogenous CENP-A depletion by siRNA treatment, of naive HeLa cells (second row) or HeLa cells stably expressing siRNA-resistant full-length GFP-CENP-A (third row) or the swapped αN_{H3}-CENP-A mutant (fourth row). On the first row are shown naive HeLa cells treated with scramble siRNA. The centromeres in naive cells were stained by CREST antibody and GFP fluorescence was used to visualize CENP-A in GFP fusion-expressing cells. An antibody against inner centromere protein (INCENP) and an anti-lamina antibody were used to detect the midbody during cytokinesis and the nuclear envelope in interphase cells (shown in red).

(D and E) Blue, DNA; quantification of the mitotic (D) and cytokinetic (E) defects at 72 hr post-transfection with siRNA against CENP-A in the indicated cell lines. For each experiment, at least 300 cells were counted. The data are means and SEM from three different experiments.

cells (Figures 7A and 7B). However, no rescue was observed in the siRNA treated stable HeLa cells expressing GFP-αN_{H3}-CENP-A since almost complete delocalization of CENP-C was observed (Figures 7A and 7B). We have further confirmed these results by using stable HeLa cells expressing either GFP-CENP-A or both GFP-αN_{H3}- CENP-A and RFP-CENP-C fusions. As expected, the absence of endogenous CENP-A in the control cells resulted in the delocalization of RFP-CENP-C and this phenotype was completely reversed by the presence of GFP-CENP-A (Figure 7C). However, only very faint RFP stained centromeres were observed in endogenous CENP-A depleted cells, stably expressing GFP-αN_{H3}-CENP-A (Figure 7C). Identical results were observed in modified MEFs depleted of CENP-A, which expressed mouse RFP-CENP-C (Figure 7D). Therefore,

the flexible CENP-A nucleosomal ends and the absence of H1 from centromeric chromatin are required for both proper CENP-C localization and function at the centromeres.

DISCUSSION

Recent X-ray diffraction studies revealed that within the crystal, the DNA ends of the CENP-A nucleosome are not firmly wrapped around the histone octamer. In this work, by using high resolution ECM, we confirmed the results of the X-ray diffraction studies and showed that in solution the CENP-A nucleosomal ends are indeed highly flexible. Our data further revealed that the uncommon structure of the αN helix of CENP-A determines this peculiar feature of the CENP-A particle. We hypothesized that
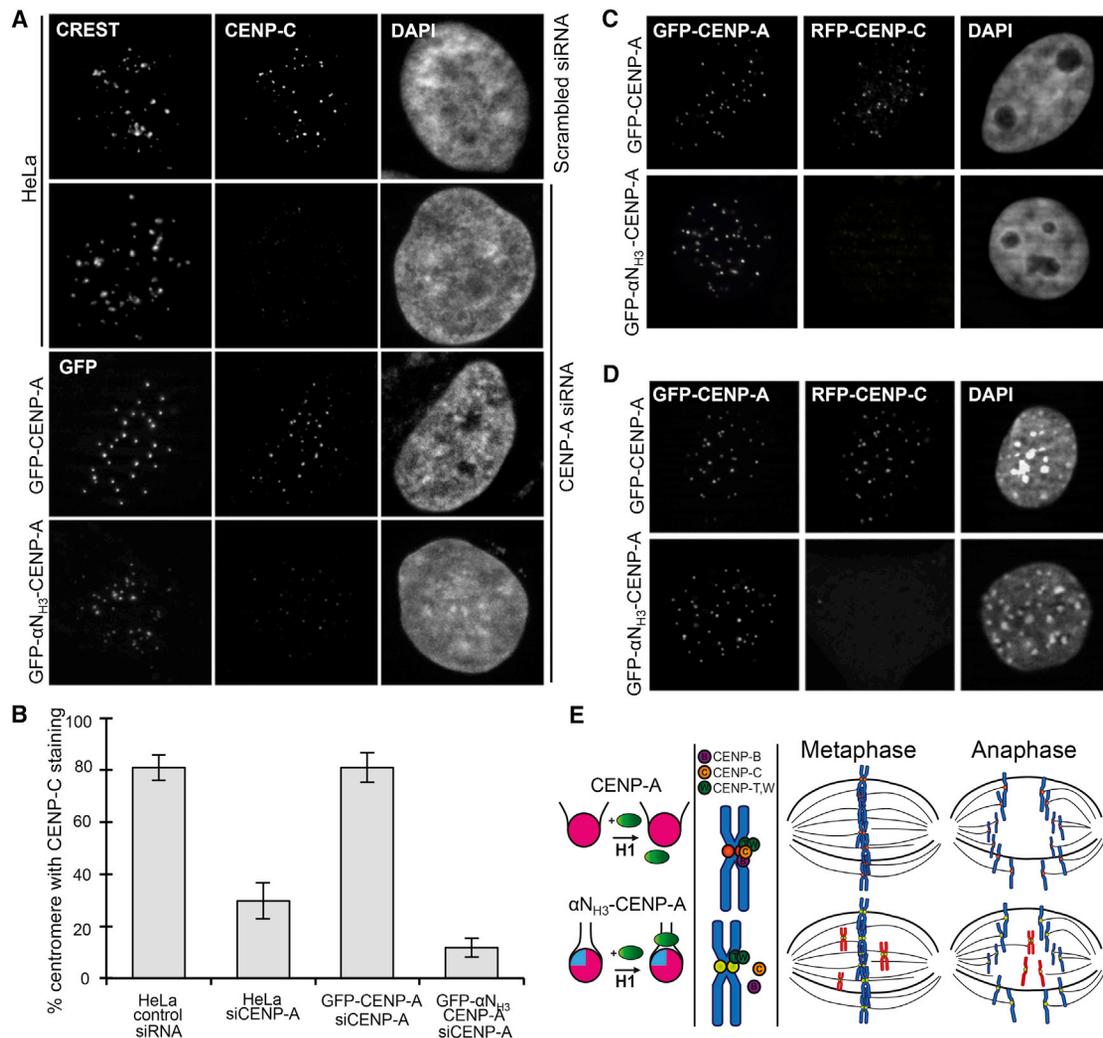
Figure 6. The Replacement in MEFs of WT CENP-A with the Swapped αN_{H3}-CENP-A Mutant at the Centromere Results in Strong Mitotic and Cytokinetic Defects

(A) Schematics of the establishment of stable MEF cell lines expressing the indicated GFP-CENP-A fusions.

(B–D) Western blot detection of the HA-GFP-CENP-A fusions and endogenous HA-CENP-A in control CENP-A (Flox/Flox) MEFs (B) and stable CENP-A (Flox/Flox) MEFs expressing either HA-GFP-CENP-A (C) or HA-GFP-αN_{H3}-CENP-A (D) at different days after tamoxifen treatment. All cells have stably inserted Cre-ERT2. H3 is used for visualization of the equal loading.

(legend continued on next page)

Figure 7. The Incorporation of Swapped αN_H3-CENP-A Mutant in the Centromeres Affects the Localization Pattern of CENP-C

(A) Immunofluorescent localization of CENP-C in CENP-A depleted HeLa cells stably expressing the indicated siRNA-resistant GFP-CENP-A fusions (rows 3 and 4). Rows 1 and 2 show the CENP-C localization in naive HeLa cells treated with scrambled or CENP-A siRNA, respectively. Centromeres in naive cells were stained with a CREST antibody.

(B) Quantification of the CENP-C delocalization data presented in (A). In each experiment, 150 cells were used. The data are means and SEM from five different experiments.

(C) Same as (A), but for the localization of the fusion RFP-CENP-C. The experiments were carried out in stable HeLa cells expressing both RFP-CENP-C and the respective siRNA-resistant GFP-CENP-A fusions.

(D) Localization of RFP-CENP-C in endogenous CENP-A-depleted MEF cells stably expressing either the GFP-CENP-A (first row) or GFP-αN_H3-CENP-A (second row) fusions.

(E) Schematics describing the role of the flexible nucleosomal ends of the CENP-A nucleosome in the organization of CENP-A centromeric chromatin and the assembly of active kinetochores. Rigidifying the ends of the CENP-A nucleosome compromises kinetochore assembly and mitosis.

maintaining DNA ends in a flexible state is central to the function of CENP-A in not only the structural context of a nucleosome, but also in the control of the biological output of CENP-A centromeric chromatin. Our results show that the higher flexibility of the DNA ends prevents the in vitro binding of the linker histone H1 to the CENP-A nucleosome. In agreement with this, no binding of H1 was observed to the CENP-A nucleosome in vivo. This observation may be linked to the fact that a stable interaction with the nucleosome requires that H1 interact not only with the DNA on the dyad axis, but also with both linker DNAs. A more

(E) Cell-cycle visualization of the effects of CENP-A depletion (8 days after the treatment with tamoxifen) in the indicated MEF lines. The first row shows the control CENP-A (Flox/Flox) MEFs, which do not have inserted Cre-ERT2.

(F and G) Quantification of the mitotic (F) and cytokinetic (G) defects in the indicated cell lines upon depletion of CENP-A after 8 days treatment with tamoxifen. For each experiment, at least 200 cells were counted. The data are means and SEM from three different experiments.

open conformation resulting in highly divergent entry and exit linker DNA ends may prevent H1 from binding simultaneously both linkers and thus weaken the interaction. Indeed, we found that hybrid H3-CENP-A nucleosome with rigid orientation of the DNA linkers was able to bind in vitro histone H1 with higher specificity and the same efficiency as conventional H3 nucleosome. In agreement with this, the in vivo replacement of the CENP-A nucleosome with rigid hybrid H3-CENP-A nucleosome led to H1 recruitment.

We have further investigated the biological outcomes of the distinct CENP-A nucleosome structure by various in vitro and in vivo approaches. Our data clearly illustrate that the highly flexible DNA ends of the CENP-A nucleosome are required for the assembly of the CCAN complex. In both HeLa and MEF cells, where the CENP-A nucleosomes were fully replaced with rigid end H3-CENP-A hybrid nucleosomes, several kinetochore proteins, including CENP-C and CENP-B, were delocalized. As a result, the kinetochore assembly was highly perturbed and the chromosome segregation was strongly affected (schematically depicted in Figure 7E). Our data thus revealed that the flexible ends of CENP-A nucleosomes are required to ensure the fidelity of the mitotic pathway in higher eukaryotes (schematically depicted in Figure 7E). The lower affinity of H1 for the CENP-A nucleosome appeared to be important for this event, since artificially induced H1 binding to centromeres, containing only rigidified hybrid H3-CENP-A nucleosomes, altered both the association of several kinetochore proteins (Figure 4; Table S2) with centromeric chromatin and the organization of the structure of the kinetochores. Since, among others, the CCAN platform protein CENP-C binds equally well to the "open" CENP-A (Guse et al., 2011; Kato et al., 2013) and rigid end hybrid H3-CENP-A particles (Figure S7A), we attribute this to the assembly of the rigid and compact conventional-like chromatin fiber containing H1 and the subsequent inability of kinetochore proteins to get access and bind to it.

Of note, the non-conventional flexible structure of the CENP-A nucleosome is likely to be preserved in all eukaryotes, including yeast (Kingston et al., 2011). All this indicates that the open structure of the CENP-A nucleosome in yeast is, as in the case of higher eukaryotes, required for mitosis. Yeast does not express, however, conventional H1 able to condense chromatin. The inability of histone H1 to bind to CENP-A nucleosomes thus allows higher eukaryotes to assemble centromeres with distinct low compact chromatin structure, which would then be important for recognition of centromeric chromatin by the kinetochore protein complexes. Therefore, evolution has preserved an open structure of CENP-A nucleosomes for chromosome segregation and mitotic fidelity.

Interestingly, CENP-A is retained quantitatively, presumably under the form of nucleosomes, in mature spermatozoa in mouse, human, and bull as well as in *Drosophila* (Hammoud et al., 2009; Palmer et al., 1990; Raychaudhuri et al., 2012). The CENP-A nucleosome as a whole is therefore likely to be inherited, thus clearly establishing the epigenetic character of the CENP-A nucleosomal structure. The flexibility of DNA ends on CENP-A nucleosome could thus be needed to establish critical protein networks important for male genome function post-fertilization.

EXPERIMENTAL PROCEDURES

Plasmids and Recombinant Protein Purification

Human silencing-resistant CENP-A and αN_{H3}-CENP-A mutants were constructed using the CENP-A coding sequence (Tanaka et al., 2004). For αN_{H3}-CENP-A construct, coding sequence of amino acids 39 to 54 from CENP-A have been replaced by coding sequence for H3.1 amino acids 38 to 53. Final CENPA constructs were cloned in frame with GFP at the N terminus into pBABE-puro vector (Addgene #1764).

Mouse αN_{H3}-CENP-A was obtained by replacing mouse CENP-A coding sequence of amino acids 34 to 49 by mouse coding sequence of H3.1 amino acids 34 to 51. Both mouse WT CENPA and mouse αN_{H3}-CENP-A were fused in N-term with HA-GFP and then cloned into retroviral pCL-MFG vector.

Human CENP-C and mouse CENP-C sequence were fused in N-ter with RFP and then cloned into pQCXIH vector (Clontech).

Construction of GFP-H3.1 and GFP-H3.3 were described elsewhere (Drané et al., 2010). Core human recombinant histones and histone H1 were expressed in bacteria and purified as described in Angelov et al. (2004) and in Syed et al. (2010), respectively. Recombinant bacterially expressed NAP-1 was purified according to the procedure described in Syed et al. (2010).

Nucleosome Reconstitution, EMSA, and ·OH Footprinting

Centrally positioned conventional or either WT CENP-A or αN_{H3}-CENP-A mono-nucleosomes and di-nucleosomes were reconstituted as described previously (Menoni et al., 2007) using 255 bp 601 DNA fragment and 2 x197 bp 601 DNA (Syed et al., 2010). The deposition of H1 was carried out by using NAP-1/H1 complexes as described in Syed et al. (2010). EMSA and ·OH footprinting were performed according to well-established protocols (Syed et al., 2010).

Cell Culture

HeLa cell lines stably expressing the various GFP-CENP-A fusions were established by retroviral infection with Moloney murine leukemia viruses (MMLV) produced by amphotropic Phoenix packaging cells (Swift et al., 2001). HeLa cell lines stably expressing either GFP-H3.1 or GFP-H3.3 were described in Drané et al. (2010). The cells were maintained in standard Dulbecco's modified Eagle's medium (DMEM) media containing 10% fetal bovine serum, 1% penicillin and streptomycin, and 1% glutamine at 37°C in a 5% CO_2 atmosphere. For generation of stable HeLa cell lines expressing FLAG-HA epitope-tagged either WT CENP-A or αN_{H3}-CENP-A swapped mutant, the cells were transfected with calcium phosphate.

Tandem Affinity Purification

The chromatin extracts were prepared from stable HeLa cell lines expressing CENP-A, αN_{H3}-CENP-A, H3.1, or H3.3 proteins fused to FLAG and HA epitope tags. The purification of both soluble and chromatin associated complexes were carried out as described in Goutte-Gattat et al. (2013) and Drané et al. (2010). After collection, cells were lysed in hypotonic buffer (10 mm Tris-HCl at pH 7.65, 1.5 mm MgCl2, and 10 mm KCl) and a Dounce homogenizer was used to disrupt them. Following incubation of the nuclear pellet in high salt buffer (final concentration of NaCl of 300 mM), tagged proteins were immunoprecipitated with anti-FLAG M2-agarose (Sigma) and eluted with FLAG peptide (0.5 mg/ml). A second step of immuno-purification was carried out with anti-HA antibody-conjugated agarose, and the material was finally eluted with HA peptide (1 mg/ml). The different complexes were separated by SDS-PAGE and stained using the Silver Quest Kit (Invitrogen). Of note, we used for proteomic analysis extracts (either nucleosomal or nuclear soluble) "normalized" to CENP-A; i.e., we first performed western blotting to evaluate the amount of CENP-A/αN_{H3}-CENP-A in the extracts and then we used either CENP-A or αN_{H3}-CENP-A extracts containing the same amount of CENP-A/αN_{H3}-CENP-A for the proteomic study. This allowed us to have some semi-quantitative estimation of the abundance of the different proteins within the complexes.

CENP-A KI-cKO Mouse Line

The CENP-A cKO/KI mouse line was established by using standard mouse genetic approaches. In this line, the CENP-A gene was replaced by a double

tagged FLAG-HA-CENP-A fusion. The targeting vector of the generated cKO/KI FLAG-HA tagged CENP-A$^{flox/flox}$ mice flanked exon 1 of the murine CENP-A gene with LoxP recombination sites. The exon 1 excision leads to the loss of expression of the protein (see Figure 4).

MEF Conditional CENP-A KO
Day 14 MEFs were isolated and cultured from CENP-A cKO/KI mice. P2 cells were immortalized and infected with MSCV CreERT2 puro (Addgene #22776) and vectors expressing CENP-A constructs. CENP-A KO is induced by adding 10 μM (Z)-4-Hydroxytamoxifen (Sigma-Aldrich) to cell culture media during 24 hr. Every 48 hr during 10 days, cells are trypsinated and a small portion of the cells is put back into culture. The rest of the cells are collected in order to perform experiments.

RNAi
Endogenous CENP-A expression was silenced by transient transfection with CENP-A siRNAs (Dharmacon). Transfections were carried out in six wells plates with 100 nM of siRNA mixed with 4 μl of Oligofectamin (Invitrogen), following the provider's instructions. The following day, the transfection medium was replaced by fresh medium and cells were allowed to grow. At 72 hr after transfection, cells were fixed on coverslip for immunofluorescence (IF) or collected for western blot.

Immunofluorescence and Microscopy Image Acquisition
Cells were fixed in formalin solution (Sigma-Aldrich) at room temperature. After permeabilization, primary antibodies were incubated in blocking buffer for 1 hr at room temperature using the following antibodies: CENP-C 1/2000^e (gift from I. Cheeseman), CREST 1/2000^e (ImmunoVision), and Lamin B 1/300^e (Santa Cruz). All microscopy was performed on fixed cells with a Zeiss Axio Imager Z1 microscope with a Plan-Apochromat ×63 objective. GFP, cyanine-2, cyanine-3, and Hoechst 33342 were used as fluorochromes. z stack images were acquired with a Zeiss Axiocam camera piloted with the Zeiss AxioVision 4.8.10 software. All image treatment was performed using Fiji (ImageJ2-rc14). For quantification of CENP-C signal at centromeres, undeconvoluted 2D maximum intensity projections were saved as 8-bit TIFF images. Each individual nucleus was determined using Hoechst staining, then colocalization of CENP-C signal with GFP-CENP-A or CREST signal was calculated using JACoP 2.1.1 plugin (Bolte and Cordelières, 2006).

ECM Image Acquisition
Specimen Preparation
The reconstituted nucleosomes were prepared in a low ionic strength buffer (10 mM Tris, 1 mM EDTA, and 10 mM NaCl) and diluted in the same buffer to a concentration of 150 mg/ml of DNA. Three microliters of the specimen were deposited on a holey carbon film (C-flat 2-2-2), rendered hydrophilic by a 20 s glow discharge in air, and flash frozen in liquid ethane using an automated plunger (Vitrobot, FEI) with controlled blotting time (1 s), blotting force (5), humidity (97%), and temperature (4°C). The particles were imaged using a cryo-transmission electron microscope (Polara, FEI) equipped with a field emission gun operating at 100 kV. Images were recorded under low-dose condition (total dose of 20 e$^-$/Å^2) on a 4096 × 4096 CCD camera (Eagle FEI) at a magnification of 59,000× resulting in a pixel size on the specimen of 0.187 nm.
Image Processing
Nucleosomal particles were selected manually using the Boxer application in the EMAN2 software package (Ludtke et al., 1999). The contrast transfer function (CTF) of the microscope was determined for each micrograph using the CTFFIND3 program (Mindell and Grigorieff, 2003). CTF correction and further image analysis was performed within the RELION software package (Scheres, 2012). The molecular images of both data sets representing conventional nucleosomes and those with incorporated CENP-A were subjected to reference-free 2D classification to remove images containing contamination or damaged particles. An initial 3D model was reconstructed from the 2D class-average images by the angular reconstitution method (Van Heel, 1987) and further refined using maximum-likelihood based methods. 3D classification was carried out to identify structural variations within the image data set. There were four or five most populated classes that were selected for each of the samples. Illus-

trations were prepared using the Chimera visualization software (Pettersen et al., 2004).

SUPPLEMENTAL INFORMATION

AUTHOR CONTRIBUTIONS

ACKNOWLEDGMENTS

REFERENCES

Angelov, D., Lenouvel, F., Hans, F., Müller, C.W., Bouvet, P., Bednar, J., Moudrianakis, E.N., Cadet, J., and Dimitrov, S. (2004). The histone octamer is invisible when NF-kappaB binds to the nucleosome. J. Biol. Chem. 279, 42374–42382.

Bednar, J., Horowitz, R.A., Grigoryev, S.A., Carruthers, L.M., Hansen, J.C., Koster, A.J., and Woodcock, C.L. (1998). Nucleosomes, linker DNA, and linker histone form a unique structural motif that directs the higher-order folding and compaction of chromatin. Proc. Natl. Acad. Sci. USA 95, 14173–14178.

Bolte, S., and Cordelières, F.P. (2006). A guided tour into subcellular colocalization analysis in light microscopy. J. Microsc. 224, 213–232.

Boulard, M., Bouvet, P., Kundu, T.K., and Dimitrov, S. (2007). Histone variant nucleosomes: structure, function and implication in disease. Subcell. Biochem. 41, 71–89.

Buscaino, A., Allshire, R., and Pidoux, A. (2010). Building centromeres: home sweet home or a nomadic existence? Curr. Opin. Genet. Dev. 20, 118–126.

Drané, P., Ouararhni, K., Depaux, A., Shuaib, M., and Hamiche, A. (2010). The death-associated protein DAXX is a novel histone chaperone involved in the replication-independent deposition of H3.3. Genes Dev. 24, 1253–1265.

Earnshaw, W.C., and Migeon, B.R. (1985). Three related centromere proteins are absent from the inactive centromere of a stable isodicentric chromosome. Chromosoma 92, 290–296.

Falk, S.J., Guo, L.Y., Sekulic, N., Smoak, E.M., Mani, T., Logsdon, G.A., Gupta, K., Jansen, L.E., Van Duyne, G.D., Vinogradov, S.A., et al. (2015). Chromosomes. CENP-C reshapes and stabilizes CENP-A nucleosomes at the centromere. Science 348, 699–703.

Foltz, D.R., Jansen, L.E., Black, B.E., Bailey, A.O., Yates, J.R., 3rd, and Cleveland, D.W. (2006). The human CENP-A centromeric nucleosome-associated complex. Nat. Cell Biol. 8, 458–469.

Goutte-Gattat, D., Shuaib, M., Ouararhni, K., Gautier, T., Skoufias, D.A., Hamiche, A., and Dimitrov, S. (2013). Phosphorylation of the CENP-A amino-terminus in mitotic centromeric chromatin is required for kinetochore function. Proc. Natl. Acad. Sci. USA 110, 8579–8584.

Guse, A., Carroll, C.W., Moree, B., Fuller, C.J., and Straight, A.F. (2011). In vitro centromere and kinetochore assembly on defined chromatin templates. Nature 477, 354–358.

Hamiche, A., Schultz, P., Ramakrishnan, V., Oudet, P., and Prunell, A. (1996). Linker histone-dependent DNA structure in linear mononucleosomes. J. Mol. Biol. 257, 30–42.

Hammoud, S.S., Nix, D.A., Zhang, H., Purwar, J., Carrell, D.T., and Cairns, B.R. (2009). Distinctive chromatin in human sperm packages genes for embryo development. Nature 460, 473–478.

Kato, H., Jiang, J., Zhou, B.R., Rozendaal, M., Feng, H., Ghirlando, R., Xiao, T.S., Straight, A.F., and Bai, Y. (2013). A conserved mechanism for centromeric nucleosome recognition by centromere protein CENP-C. Science 340, 1110–1113.

Kingston, I.J., Yung, J.S., and Singleton, M.R. (2011). Biophysical characterization of the centromere-specific nucleosome from budding yeast. J. Biol. Chem. 286, 4021–4026.

Ludtke, S.J., Baldwin, P.R., and Chiu, W. (1999). EMAN: semiautomated software for high-resolution single-particle reconstructions. J. Struct. Biol. 128, 82–97.

Luger, K., Mäder, A.W., Richmond, R.K., Sargent, D.F., and Richmond, T.J. (1997). Crystal structure of the nucleosome core particle at 2.8 A resolution. Nature 389, 251–260.

Makarov, V.L., Dimitrov, S.I., and Petrov, P.T. (1983). Salt-induced conformational transitions in chromatin. A flow linear dichroism study. Eur. J. Biochem. 133, 491–497.

Menoni, H., Gasparutto, D., Hamiche, A., Cadet, J., Dimitrov, S., Bouvet, P., and Angelov, D. (2007). ATP-dependent chromatin remodeling is required for base excision repair in conventional but not in variant H2A.Bbd nucleosomes. Mol. Cell. Biol. 27, 5949–5956.

Menoni, H., Shukla, M.S., Gerson, V., Dimitrov, S., and Angelov, D. (2012). Base excision repair of 8-oxoG in dinucleosomes. Nucleic Acids Res. 40, 692–700.

Mindell, J.A., and Grigorieff, N. (2003). Accurate determination of local defocus and specimen tilt in electron microscopy. J. Struct. Biol. 142, 334–347.

Mizuguchi, G., Xiao, H., Wisniewski, J., Smith, M.M., and Wu, C. (2007). Nonhistone Scm3 and histones CenH3-H4 assemble the core of centromere-specific nucleosomes. Cell 129, 1153–1164.

Palmer, D.K., O'Day, K., Wener, M.H., Andrews, B.S., and Margolis, R.L. (1987). A 17-kD centromere protein (CENP-A) copurifies with nucleosome core particles and with histones. J. Cell Biol. 104, 805–815.

Palmer, D.K., O'Day, K., and Margolis, R.L. (1990). The centromere specific histone CENP-A is selectively retained in discrete foci in mammalian sperm nuclei. Chromosoma 100, 32–36.

Perpelescu, M., and Fukagawa, T. (2011). The ABCs of CENPs. Chromosoma 120, 425–446.

Pettersen, E.F., Goddard, T.D., Huang, C.C., Couch, G.S., Greenblatt, D.M., Meng, E.C., and Ferrin, T.E. (2004). UCSF Chimera–a visualization system for exploratory research and analysis. J. Comput. Chem. 25, 1605–1612.

Raychaudhuri, N., Dubruille, R., Orsi, G.A., Bagheri, H.C., Loppin, B., and Lehner, C.F. (2012). Transgenerational propagation and quantitative maintenance of paternal centromeres depends on Cid/Cenp-A presence in Drosophila sperm. PLoS Biol. 10, e1001434.

Régnier, V., Vagnarelli, P., Fukagawa, T., Zerjal, T., Burns, E., Trouche, D., Earnshaw, W., and Brown, W. (2005). CENP-A is required for accurate chromosome segregation and sustained kinetochore association of BubR1. Mol. Cell. Biol. 25, 3967–3981.

Scheres, S.H. (2012). RELION: implementation of a Bayesian approach to cryo-EM structure determination. J. Struct. Biol. 180, 519–530.

Shuaib, M., Ouararhni, K., Dimitrov, S., and Hamiche, A. (2010). HJURP binds CENP-A via a highly conserved N-terminal domain and mediates its deposition at centromeres. Proc. Natl. Acad. Sci. USA 107, 1349–1354.

Shukla, M.S., Syed, S.H., Goutte-Gattat, D., Richard, J.L., Montel, F., Hamiche, A., Travers, A., Faivre-Moskalenko, C., Bednar, J., Hayes, J.J., et al. (2011). The docking domain of histone H2A is required for H1 binding and RSC-mediated nucleosome remodeling. Nucleic Acids Res. 39, 2559–2570.

Song, F., Chen, P., Sun, D., Wang, M., Dong, L., Liang, D., Xu, R.M., Zhu, P., and Li, G. (2014). Cryo-EM study of the chromatin fiber reveals a double helix twisted by tetranucleosomal units. Science 344, 376–380.

Swift, S., Lorens, J., Achacoso, P., and Nolan, G.P. (2001). Rapid production of retroviruses for efficient gene delivery to mammalian cells using 293T cell-based systems. Curr. Protoc. Immunol. http://dx.doi.org/10.1002/0471142735.im1017cs31.

Syed, S.H., Goutte-Gattat, D., Becker, N., Meyer, S., Shukla, M.S., Hayes, J.J., Everaers, R., Angelov, D., Bednar, J., and Dimitrov, S. (2010). Single-base resolution mapping of H1-nucleosome interactions and 3D organization of the nucleosome. Proc. Natl. Acad. Sci. USA 107, 9620–9625.

Tachiwana, H., Kagawa, W., Shiga, T., Osakabe, A., Miya, Y., Saito, K., Hayashi-Takanaka, Y., Oda, T., Sato, M., Park, S.Y., et al. (2011). Crystal structure of the human centromeric nucleosome containing CENP-A. Nature 476, 232–235.

Tanaka, Y., Tawaramoto-Sasanuma, M., Kawaguchi, S., Ohta, T., Yoda, K., Kurumizaka, H., and Yokoyama, S. (2004). Expression and purification of recombinant human histones. Methods 33, 3–11.

Thoma, F., Koller, T., and Klug, A. (1979). Involvement of histone H1 in the organization of the nucleosome and of the salt-dependent superstructures of chromatin. J. Cell Biol. 83, 403–427.

Van Heel, M. (1987). Angular reconstitution: a posteriori assignment of projection directions for 3D reconstruction. Ultramicroscopy 21, 111–123.

Van Holde, K.E., Allen, J.R., Tatchell, K., Weischet, W.O., and Lohr, D. (1980). DNA-histone interactions in nucleosomes. Biophys. J. 32, 271–282.

Zhou, B.R., Feng, H., Kato, H., Dai, L., Yang, Y., Zhou, Y., and Bai, Y. (2013). Structural insights into the histone H1-nucleosome complex. Proc. Natl. Acad. Sci. USA 110, 19390–19395.

Zhou, B.R., Jiang, J., Feng, H., Ghirlando, R., Xiao, T.S., and Bai, Y. (2015). Structural mechanisms of nucleosome recognition by linker histones. Mol Cell 59, 628–638.